

# Specific Force Deficit in Skeletal Muscles of Old Rats Is Partially Explained by the Existence of Denervated Muscle Fibers

Melanie G. Urbanek,<sup>1</sup> Elisa B. Picken,<sup>2</sup> Loree K. Kalliainen,<sup>3</sup> and William M. Kuzon, Jr.<sup>1,4</sup>

<sup>1</sup>Division of Plastic and Reconstructive Surgery, University of Michigan, Ann Arbor.

<sup>2</sup>Mayo Medical School, Rochester, Minnesota.

<sup>3</sup>Division of Plastic Surgery, Ohio State University, Columbus.

<sup>4</sup>Department of Veterans Affairs Medical Center, Ann Arbor, Michigan.

**We tested the hypothesis that denervated muscle fibers account for part of the specific force ( $sF_o$ ) deficit observed in muscles from old adult (OA) mammals. Whole muscle force ( $F_o$ ) was quantified for extensor digitorum longus (EDL) muscles of OA and young adult (YA) rats. EDL muscle  $sF_o$  was calculated by dividing  $F_o$  by either total muscle fiber cross-sectional area (CSA) or by innervated fiber CSA. Innervated fiber CSA was estimated from EDL muscle cross sections labeled for neural cell adhesion molecules, whose presence is a marker for muscle fiber denervation. EDL muscles from OA rats contained significantly more denervated fibers than muscles from YA rats (5.6% vs 1.1% of total CSA). When compared with YA muscle, OA muscle demonstrated deficits of 34.1% for  $F_o$ , 28.3% for  $sF_o$ , and 24.9% for  $sF_o$  calculated by using innervated CSA as the denominator. Denervated muscle fibers accounted for 11.3% of the specific force difference between normal YA and OA skeletal muscle. Other mechanisms in addition to denervation account for the majority of the  $sF_o$  deficit with aging.**

THE age-associated skeletal muscle weakness found in humans and rodents is disproportionate to the degree of age-associated loss in muscle mass and fiber area (1–10). Atrophy and loss of muscle fibers explain part of the age-associated force deficit seen in some muscles, but when relative force calculations are adjusted for the decrease in muscle mass, a deficit in specific force ( $sF_o$ ) is noted for the fast-twitch extensor digitorum longus (EDL) and plantaris muscles (1,3,6) and slow-twitch soleus (11). This age-associated muscle weakness is not due to a reduced supply of energy transduction metabolites (phosphocreatine, adenosine triphosphate, adenosine diphosphate) or to intrinsic force-generating capacity impairment of the cross bridges (4,8). Changes in the excitation–contraction coupling mechanism are documented in intact single fiber studies, indicating failure of the sarcoplasmic reticulum to present enough calcium for complete activation (12,13); however, others find no activation failure when using twitch interpolation to full activation (7). Spontaneous denervation occurs normally in aging muscle as seen by a reduction in the average number of motor units, motor units occupying larger territories and displaying larger innervation ratios, and a nonrandom arrangement of motor unit fibers in some muscles of old animals (14–19). We hypothesize that the loss of specific force seen in senescent muscle may be partially explained by denervated muscle fibers resulting from age-associated spontaneous denervation.

Muscle fiber surface and intracellular accumulation of the integral membrane glycoprotein neural cell adhesion molecule (NCAM) is a general response to muscle denervation (20,21). Increased levels of the total amount of NCAM protein and of NCAM mRNA are observed in denervated skeletal muscle (16,17,21). Immunohistochemically detectable

NCAM appears within 2 days of denervation and remains elevated for up to 300 days in muscle that is kept denervated (20). The NCAM is not uniquely associated with either fast-twitch (type II) or slow-twitch (type I) fibers (20). NCAM is undetectable on large adult normal myelinated axons but is present on the unmyelinated terminals and synaptic portions of adult neuromuscular junctions (20,22). NCAM is undetectable at portions of normal innervated muscle fibers distant from synapses (22). Thus differentiation between denervated and innervated muscle fibers is possible by using NCAM immunohistochemistry, because only denervated fibers express NCAM in the extrajunctional sarcolemma.

We examined the effect of aging on EDL muscle maximal force-generating capacity relative to muscle fiber denervation. Two age groups of EDL muscle were compared. A group of 3-month-old rats represented the young adult (YA) age group, whereas 27- to 29-month-old rats represented the old age (OA) group.

We confirmed the existence of a force deficit and a specific force deficit when the forces are normalized to account for reduced total muscle fiber cross-sectional area (CSA) in the OA group EDL muscle maximal force-generating capacity when compared with that of our YA group (1–10). A further reduction in the deficit between the YA and OA groups is anticipated by correcting the EDL muscle CSA for denervated fibers, which exist as part of the CSA but which do not contribute to in situ force production. That is, the  $sF_o$  deficit in muscle from OA compared with that from YA animals will be reduced by using only the CSA for innervated fibers when the specific force ( $sF_o$  innervated) is calculated. We tested the hypothesis that the specific force deficit observed in skeletal muscles of old animals is at least partially

accounted for by a higher percentage of denervated muscle fibers in muscles from old than in muscles from young animals. If denervated fibers are the only mechanism contributing to the specific force deficit in muscles from old animals,  $sF_o$  innervated will not differ between muscles from animals in the YA and the OA groups.

To test this hypothesis we determined the maximal isometric force of the EDL muscle in YA and OA rats. We calculated the CSA of each muscle and also estimated innervated and denervated CSA for each muscle by using histological techniques that combined NCAM labeling with morphometric planimetry measurements (23–25). For each group, EDL muscle  $sF_o$  and  $sF_o$  innervated were calculated by using either the total or the innervated muscle fiber CSA as the normalizing variable.

## METHODS AND MATERIALS

We studied a YA group of 3-month-old ( $n = 5$ ) and an OA group of 27- to 29-month-old ( $n = 7$ ) male specific pathogen-free Fischer 344 (F344) rats (Charles River Laboratory; Portage, MI). All procedures were approved by the Institutional Animal Care and Use Committee at the University of Michigan and were in strict accordance with the National Research Council's guide for the care and use of laboratory animals (26). The rats were certified as being specific pathogen free at the time of delivery. They were maintained for 7–25 days in a barrier facility that continued enforcement of specific pathogen precautions. On a quarterly basis, University Laboratory Animal Medicine personnel verified that colony rats were free from specific viruses, Sendai, and *Mycoplasma pulmonis*. Rodent chow and water were available ad libitum. Rats were individually housed and were free to move about their cages.

### Muscle Function Evaluation

Rats were anesthetized with an initial intraperitoneal injection of pentobarbital sodium 65 mg/kg. Supplemental injections were given as necessary to maintain a deep plane of anesthesia. Evaluations were performed on EDL muscle in only the left leg of each rat. The peroneal nerve was exposed through a muscle-splitting incision in the hip. Skin flaps in the leg were elevated. The tibialis anterior muscle was elevated by cutting the distal tendon. The EDL muscle was exposed while the neurovascular pedicle was carefully preserved. The four distal EDL muscle tendons were transected in the foot and gently drawn through the transverse ligament at the ankle. The tendons were looped and tied distal to the musculotendinous junction. The leg was rigidly stabilized at the knee by using a Kirschner pin and at the ankle with a foot clamp. The tendon loop was attached directly to the lever arm of a servomotor (Model 305, Cambridge Technology, Cambridge, MA), keeping the EDL muscle in parallel with the tibia. The rat was placed on a platform maintained at 37°C by a circulating water bath.

Throughout the evaluation, the peroneal nerve and EDL muscle and tendon temperatures were maintained at 35°C with warmed mineral oil. Supramaximal stimulation between 3 and 12 V was delivered in square wave pulses lasting 0.2 milliseconds generated by a Grass S88 stimulator (Grass Instrument Co., Quincy, MA) through shielded stainless-steel

electrodes placed around the peroneal nerve (Harvard Apparatus, South Natick, MA; 27). This activated only the EDL muscle, as nerve branches to all surrounding muscles were severed to minimize extraneous motion artifacts. Tensions between 50 and 5000 mN could be recorded reliably.

Maximal isometric tetanic tension ( $F_o$ , in millinewtons), also known as maximal force capacity, was quantified for the EDL muscle by using established methods (25). The servomotor arm position was controlled by a microcomputer (Dell Computer Corp., Austin, TX) that was equipped with a digital-to-analog converter (Data Translation, Marlboro, MA) and appropriate custom software (ASYST Software Technologies, Inc., Rochester, NY). The servomotor arm was maintained at a constant position during force measurement. Position and force were monitored and displayed on a storage oscilloscope (Gould Inc., Romulus, MI). The microcomputer sampled force data during contractions via analog-to-digital channels. The stimulation voltage was increased each trial, beginning at 1 V, until a maximal twitch response was reached. This maximal twitch voltage was subsequently delivered for isometric force measurements. Muscle length was adjusted until the isometric twitch contraction force was maximized. This adjusted muscle length was defined as the optimum muscle length ( $L_o$ ) for force production. With the muscle held at  $L_o$  and with the use of maximal twitch voltage, the stimulation train duration was increased to 350 milliseconds for measurements of maximal force. In sequential trials to pinpoint maximum force, the stimulation frequency was incremented from 50 to 200 Hz while the stimulation pulse width was held constant at 0.2 milliseconds. A 3-minute recovery was imposed between each contraction measurement. Upon completion of testing, the muscle was further exposed above the knee,  $L_o$  was directly measured from the most proximal to most distal muscle fiber tissue by using calipers, the EDL muscle was harvested, tendons were trimmed, and the muscle was weighed and frozen in isopentane cooled to  $-160^\circ$  with liquid nitrogen. The frozen muscles were stored for histochemical processing.

The average ratio of fiber length to muscle length ( $L_f/L_m$ ) was determined by using nitric acid digestion (28–30). The contralateral, right EDL muscle for three rats in the OA group and for six additional same strain, F344, male rats aged 5 to 7 months were also surgically exposed for direct  $L_m$  measurement from the most proximal to most distal muscle fiber tissue. The ankle and knee joints were held at  $90^\circ$  during measurement. The contralateral EDL muscle was surgically removed and digested with nitric acid for muscle fiber length measurement and  $L_f/L_m$  calculation. Each rat was euthanized with an overdose of pentobarbital sodium.

### Immunofluorescent Labeling of NCAM Protein

Binding of antibodies to tissue sections was detected by use of an immunofluorescent method (31). Cross sections of unfixed EDL muscle were cut from the middle one third of the muscle at 12  $\mu\text{m}$  in a  $-30^\circ\text{C}$  cryostat, air dried on poly-L-lysine coated glass slides, and fixed with methanol for 2–5 minutes at  $-10^\circ\text{C}$ . Sections were incubated successively with 2–5% goat serum in phosphate-buffered saline (PBS)

followed by 5  $\mu\text{g}/\text{ml}$  of affinity-purified polyclonal anti-NCAM (Chemicon, Temecula, CA; AB1505, rabbit, antirat, human, mouse, and ox) as the primary antibody. After a pH 7.4 PBS wash, sections were incubated with 12.5  $\mu\text{g}/\text{ml}$  of rhodamine-conjugated goat antirabbit IgG F(ab')<sub>2</sub> fragments (American Qualix, La Mirada, CA) as the secondary antibody, then washed again with pH 7.4 PBS and mounted in glycerol containing paraphenylamine diamine (ICN stock, pH 8.0; see Ref. 22). Fluorescein-labeled  $\alpha$ -bungarotoxin at 10  $\mu\text{g}/\text{ml}$  (Sigma Chemicals, St. Louis, MO), which binds to acetylcholine receptors in the postsynaptic membrane, was mixed with the secondary antibody to identify motor endplates. Duplicate "blank" slides were processed in which 10% bovine serum albumin (BSA) in PBS was substituted for affinity-purified polyclonal anti-NCAM.

Sections were illuminated and photographed (Yashika 35-mm camera, Kyocera Corp., Tokyo, Japan) as magnified 32 $\times$  through a Leitz Laborlux S fluorescent microscope (Leica, Wetzlar, Germany) through filters selective for either Fluorescein (BP 450–490) or Rhodamine (BP 515–560). After immunofluorescent labeling and photography, photographs were digitized to compact disk; the images were reassembled into a complete muscle cross section by using Adobe Photoshop software (Mountain View, CA). Individual cells that bound anti-NCAM antibody and did not bind  $\alpha$ -bungarotoxin were classified as NCAM positive (NCAM<sup>+</sup>); the rest

of the cells were classified as NCAM negative (NCAM<sup>-</sup>; see Figure 1). A muscle fiber was defined as denervated if it labeled positively for NCAM and negatively for  $\alpha$ -bungarotoxin. We measured the CSA for all individual cells in each EDL cross section with digital planimetry software (Sigma-Scan, Jandel, San Raphael, CA). NCAM<sup>+</sup> and NCAM<sup>-</sup> fiber counts were totaled during planimetry as all fibers were measured and classified in each typical cross section. NCAM<sup>+</sup>CSA was the total CSA for all NCAM<sup>+</sup> labeled fibers in a cross section as measured with planimetry. NCAM<sup>-</sup>CSA was the total CSA for all NCAM<sup>-</sup> labeled fibers in a cross section as measured with planimetry.

The mean "physiological" CSA was determined by dividing the muscle wet mass (milligrams) by the product of  $L_f$  (millimeters) and 1.06  $\text{g cm}^{-3}$  which is the density of mammalian skeletal muscle (23,32); see Equation (1). Specific  $F_o$  ( $sF_o$ ) was calculated by dividing  $F_o$  by the physiological CSA; see Equation (2). As NCAM<sup>+</sup> muscle fibers were considered to be denervated, the relative total area of NCAM<sup>-</sup> fibers in each section was considered to represent the potentially contractile CSA percent,  $\text{CSA}_{\text{innervated}}(\%)$ , given in Equation (3). A specific force ( $sF_o_{\text{innervated}}$ ) per innervated CSA (kilonewtons per square meter) was based on  $\text{CSA}_{\text{innervated}}(\%)$ , as shown in Equation (4). In Equation (4), the denervated wet muscle mass is assumed to have the same density as the innervated muscle. The proportion of

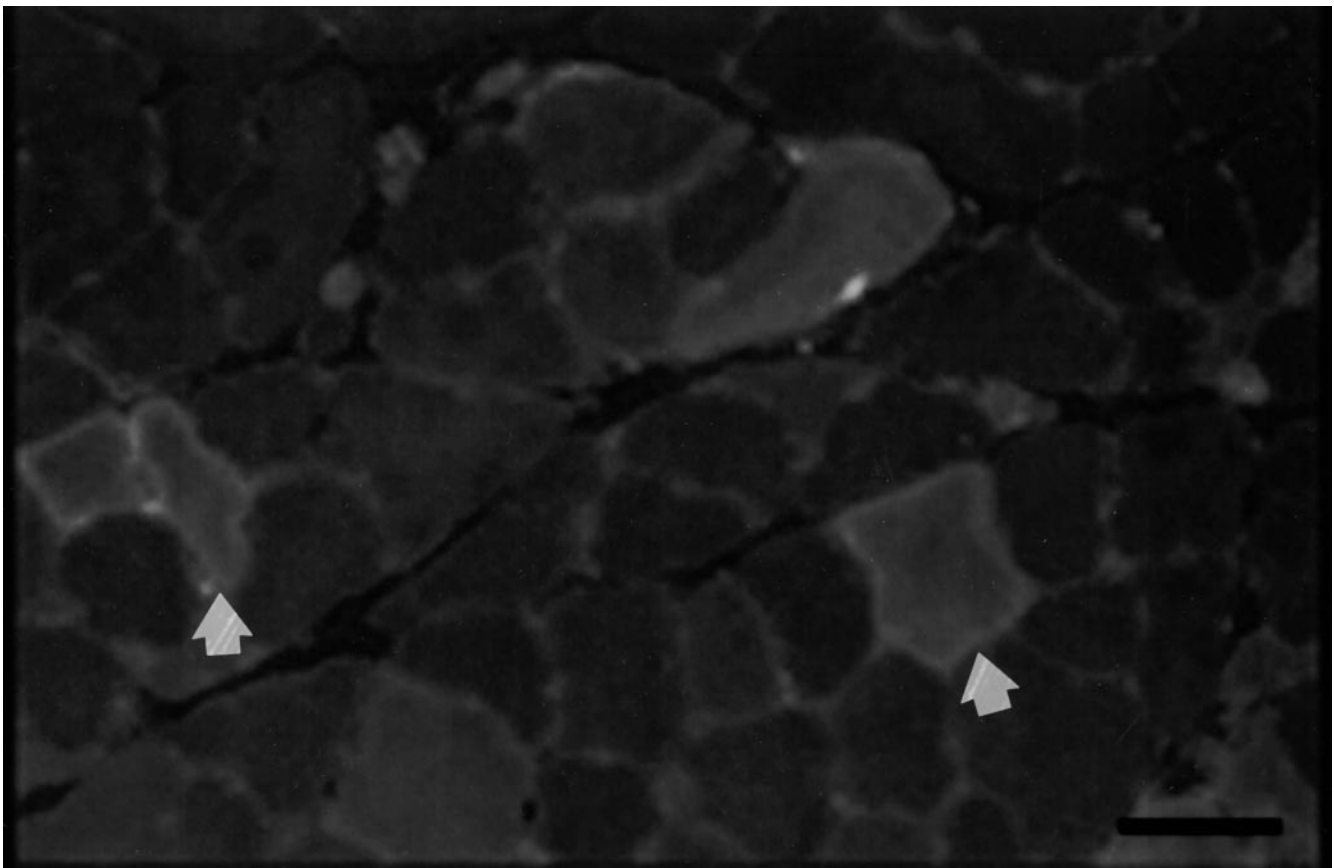


Figure 1. Photomicrograph of extensor digitorum longus muscle cross section from an old adult rat. Arrows indicate example fibers that labeled positively for NCAM protein. The fluorescent label was Rhodamine. Scale bar is 100  $\mu\text{m}$ .

the  $sF_o$  deficit in the EDL muscles of OA rats that could be accounted for by the presence of denervated fibers was calculated according to Equation (5). Physiological CSA,  $sF_o$ ,  $CSA_{innervated}$  (%), and  $sF_o_{innervated}$  were calculated by using  $F_o$  and digitized data for all EDL muscles. Equation (5) was calculated by using mean values.

$$\text{physiological CSA} = \frac{\text{mmass} \times \cos\theta}{\rho L_o 0.35} \quad (1)$$

where

physiological CSA is the muscle fiber CSA, mmass is the muscle mass,

$\theta$  is the angle of pennation for rat EDL muscle (less than  $3^\circ$ ),  $\rho$  is the density of mammalian skeletal muscle ( $1.06 \text{ g/cm}^3$ ),  $L_o$  is the optimal muscle length for force production, and 0.35 is the measured  $L_f/L_m$  ratio for rat EDL muscle.

$$sF_o (\text{kN/m}^2) = \frac{F_o}{\text{physiological CSA}} \quad (2)$$

where

$sF_o$  is the maximal specific force and  $F_o$  is the maximal tetanic force.

$$CSA_{innervated}(\%) = \frac{(\text{NCAM}^- \text{CSA})}{(\text{NCAM}^- \text{CSA} + \text{NCAM}^+ \text{CSA})} \times 100 \quad (3)$$

where

$CSA_{innervated}(\%)$  is the percentage of CSA considered to be innervated,

NCAM<sup>-</sup>CSA is the digitized CSA that is negative for NCAM protein (innervated), and

NCAM<sup>+</sup>CSA is the digitized CSA that is positive for NCAM protein (denervated).

$$sF_o_{innervated} = \frac{F_o}{\text{physiological CSA}} \times \frac{(\text{NCAM}^- \text{CSA} + \text{NCAM}^+ \text{CSA})}{(\text{NCAM}^- \text{CSA})} \quad (4)$$

where  $sF_o_{innervated}$  normalizes each  $F_o$  to only the percentage of physiological CSA, which is innervated by multiplying the physiological CSA by the percent of CSA that is innervated.

$\% \Delta sF_o =$

$$\left[ \frac{(sF_o_{o,YA} - sF_o_{o,OA}) - (sF_o_{innervated,YA} - sF_o_{innervated,OA})}{sF_o_{o,YA} - sF_o_{o,OA}} \right] \times 100, \quad (5)$$

where

$\% \Delta sF_o$  is the proportion of  $sF_o$  deficit that can be accounted for by denervated muscle fibers,

$sF_o_{o,YA}$  is the mean  $sF_o$  specific for YA by using physiological CSA,

$sF_o_{o,OA}$  is the mean  $sF_o$  specific for OA by using physiological CSA,

$sF_o_{innervated,YA}$  is the mean  $sF_o$  specific for YA by using innervated CSA only, and

$sF_o_{innervated,OA}$  is the mean  $sF_o$  specific for OA by using innervated CSA only.

### Statistical Analysis

The dependent variable of critical interest in this study is maximal isometric force capacity for the EDL muscle. In a previous study, similarly aged F344 rat EDL measurements for  $F_o$  were measured by this laboratory (33). From previous data (33), we determined that a mean  $F_o$  difference of  $600 \text{ mN} \pm 400 \text{ mN}$  between groups with numbers of 5 and 7 was physiologically significant. A statistical power analysis, Pass 6.0 (NCSS, Kaysville, UT), using this data predicted the available power for a  $t$ -test comparison between means using a one-tailed test to determine that the critical limits would be 79% ( $\alpha < 0.05$ ). A one-tailed test was selected as we predict that the  $F_o$  for the OA group is less than the  $F_o$  for the YA group (1–10).

Raw data were tested for normality (SigmaStat, SPSS Inc., Chicago, IL) by using Kolmogorov–Smirnov test distances and  $p$  values of .05. Statistical tests were performed by using SAS for Windows (SAS Institute Inc., Cary, NC). The mean and standard deviation (SD) were determined for each variable by age group. An  $\alpha$ -level equal to 0.05 was selected a priori as being appropriately stringent. A general linear model (GLM) analysis determined the significance of the differences between the measured dependent variables of body mass, muscle descriptive variables, and  $F_o$ , in the YA versus OA age groups. As the OA group CSA and CSA<sup>+</sup> data were not normally distributed, a non-parametric, Mann–Whitney  $U$  test was used to compare group means for force variables that were normalized to CSA or CSA<sup>+</sup> and all histological data. For all comparisons, two-tailed tests of the alternative hypotheses were applied.

### RESULTS

Five YA and seven OA rats successfully completed the study; the mean age was 3 months for the YA group and 28.4

Table 1. Summary for Descriptive EDL Muscle Data for YA and OA Fischer 344 Rats

Parameter	YA (n = 5)	OA (n = 7)	Change (%)	Significance
Body mass (g)	326 ± 14	374 ± 48	+15	NS*
Muscle mass (mg)	150 ± 17	148 ± 25	-1	NS*
$L_o$ (mm)	32 ± 1	34 ± 2	+6	NS*
$L_m$ (mm)*	33 ± 1	33 ± 1	0	NS*
$L_f$ (mm)	11 ± 0.3	12 ± 1	+9	NS*
EDL CSA (mm <sup>2</sup> )	13 ± 1	12 ± 2	-8	NS†

Notes:  $L_o$  = optimal muscle length;  $L_m$  = muscle length;  $L_f$  = muscle fiber length; EDL = extensor digitorum longus muscle; CSA = cross-sectional area; NS = not significant. Data are means ± SD. Statistical tests are significant at  $p < .05$ , Young Adult (YA) vs Old Adult (OA) in a two-tailed test. Mean ages were YA = 3 months and OA = 28.4 months.

\*A general linear models procedure is indicated.

†A Mann–Whitney  $U$  test is indicated.

Table 2. In Situ EDL Muscle Contractile Force Properties for YA and OA Fischer 344 Rats

Parameter	YA (n = 5)	OA (n = 7)	Change (%)	Significance
$F_o$ (mN)	3290 ± 320	2170 ± 490	-34	$p < .05^*$
$sF_o$ (kN/m <sup>2</sup> )	259 ± 18	186 ± 47	-28	$p < .05^\dagger$
$sF_o$ innervated (kN/m <sup>2</sup> )	262 ± 17	197 ± 50	-25	$p < .05^\dagger$

Notes:  $F_o$  = maximal tetanic muscle force;  $sF_o$  = maximal specific force;  $sF_o$  innervated =  $F_o$  normalized to innervated muscle fiber physiologic cross-sectional area; EDL = extensor digitorum longus muscle. Values are means ± SD. Statistical tests are significant at  $p < .05$ , Young Adult (YA) vs Old Adult (OA) in a two-tailed test. Mean ages were YA = 3 months and OA = 28.4 months.

\*A general linear models is indicated.

†A Mann-Whitney  $U$  test is indicated.

months for the OA group. Descriptive morphology data (mean ± SD) are summarized in Table 1. No significant effect of aging was observed between the YA group and the OA group for body mass or for EDL muscle mass, CSA,  $L_o$ , and  $L_f$ . Nitric acid digestion completed for the EDL muscle from YA rats (5- to 7-month-old rats) and the OA group showed that mean fiber lengths were 35% of  $L_o$  for both groups. The 5- to 7-month-old group closely resembles the 3-month-old YA group in average muscle mass and  $L_m$  (158.5 mg, 150.8 mg and 33.2 mm, 32.0 mm, respectively) but no force data were collected for the 5- to 7-month-old group.

The in situ force measurements are summarized in Table 2. Age had a significant effect in all statistical comparisons of mean force values, that is,  $F_o$ ,  $sF_o$ , and  $sF_o$  innervated. The OA group developed absolute  $F_o$ , which was 34.1% lower than the YA group. When forces were normalized for EDL muscle CSA, the  $sF_o$  remained 28.3% lower for the OA group compared with that for the YA group. When further corrections adjusted normalized force to reflect only the innervated muscle fiber CSA, the  $sF_o$  innervated deficit in the OA group was 24.9% compared with that of the YA group. Thus a deficit in specific force attributable to aging remained after normalizing for muscle fiber denervation.

The NCAM histological data are summarized in Table 3. There was no effect of age on the total absolute CSA or the total number of EDL muscle fibers counted in each age group. Aging did significantly affect the percentage of fibers that were NCAM<sup>+</sup>. The number of fibers that were NCAM<sup>+</sup> in each EDL muscle was significantly increased in the OA muscle group. In summary, aging affected a significant increase in the percentage of EDL muscle CSA that was denervated. Accounting for increases in denervated fiber CSA in the OA group did not equalize its  $sF_o$  innervated to that of the YA group. We were able to attribute 11.3% of the  $sF_o$  deficit seen between the normal YA group and the OA group to muscle fiber denervation; see Equation (5).

## DISCUSSION

Under the conditions of our experiment, 11.3% of the  $sF_o$  deficit in the old EDL muscles was accounted for by the presence of denervated muscle fibers. We hold tenable our stated hypothesis that the loss of specific force seen in senescent muscle may be partially explained by denervated muscle fibers. This was a fixed effects model in that only maximal forces or maximal specific forces and only two age groups were analyzed. Neither our force measurements nor our age groups are considered to be random, and thus our results cannot be generalized to submaximal forces or other ages.

Normal adult rodent muscle extract contains very low levels of NCAM (34). The percentage of NCAM<sup>+</sup>CSA for our YA group was only 1.1%. Studies report that a significant upregulation in muscle NCAM mRNA patterns occurs during aging (17). Though abundantly distributed across embryonic and perinatal muscle fibers, NCAM becomes colocalized with the acetylcholine receptor at the neuromuscular junction upon fiber innervation (22,35). NCAM reappears within muscle fibers, on muscle fiber surfaces, and on cells in interstitial spaces when muscle is denervated or pharmacologically paralyzed (20,35). The reappearance of NCAM protein continues as long as the muscle is denervated, for as long as 10 months, though there is some de-

Table 3. Histological Data Summary for YA and OA Fischer 344 Rat EDL Muscle, Labeled for NCAM Protein

Parameter	Group		Change (%)	Significance
	YA (n = 5)	OA (n = 7)		
CSA <sub>innervated</sub> (mm <sup>2</sup> )	13 ± 1	11 ± 2	-15	NS
NCAM <sup>+</sup> fiber count (%)	1 ± 1	8 ± 2	+700	$p < .05$
NCAM <sup>-</sup> CSA (%)				
CSA <sub>innervated</sub> (%)	99 ± 1	94 ± 2	-5	$p < .05$
NCAM <sup>+</sup> CSA (%)				
CSA <sub>denervated</sub> (%)	1 ± 1	6 ± 2	+500	$p < .05$
NCAM <sup>+</sup> individual fiber area (μm <sup>2</sup> )*	4000 ± 250	1680 ± 520	-58	$p < .05$
NCAM <sup>-</sup> individual fiber area (μm <sup>2</sup> )	3240 ± 520	2420 ± 620	-25	$p < .05$
Total fiber count <sup>†</sup>	1510 ± 110	1180 ± 400	-22	NS
NCAM <sup>+</sup> fiber count	15 ± 15	93 ± 40	+520	$p < .05$
NCAM <sup>-</sup> fiber count	1500 ± 100	1090 ± 370	-27	NS

Notes: CSA = physiological cross-sectional area; EDL = extensor digitorum longus muscle; NCAM = neural cell adhesion molecule; CSA<sub>innervated</sub> = innervated CSA (total muscle CSA not positively labeled with NCAM protein CSA); NCAM<sup>+</sup> = labeled positively for NCAM protein; NCAM<sup>-</sup> = labeled negatively for NCAM protein. Data are mean ± SD. Differences between Young Adult (YA) vs Old Adult (OA) groups were tested with the Mann-Whitney  $U$  test. Statistical significance of  $p < .05$  is by a two-tailed test. NS indicates not statistically significant. Mean ages were YA = 3 months and OA = 28.4 months.

\*Only three muscles in the YA group had NCAM<sup>+</sup> fibers.

†Comparison was based on YA (n = 4), OA (n = 7).

crease in detection (20,34). The increase in muscle extract, NCAM protein is 10-fold at 10 days post denervation but only threefold by 4 months of denervation (34). Our study found a significant increase (reappearance) equal to 409.1% for the aged, OA muscle NCAM<sup>+</sup>CSA relative to the YA group. When muscle is reinnervated, the denervation-induced accumulation of NCAM protein is reversed (20). By labeling EDL muscle for the presence of NCAM, we were able to directly demonstrate an increased number of denervated fibers in the muscles of old, compared with young, rats. However, in OA muscle, a fiber may be denervated longer than the time when NCAM expression is known to be dramatically upregulated, and we may have underestimated the number of denervated fibers, the NCAM<sup>+</sup>CSA, and the percentage of  $sF_o$  deficit that could be attributed to denervated fibers in the OA group.

Though NCAM is necessary for axonal sprouting, it is not necessary for synaptic development (36,37). Increased NCAM expression occurs in muscles that show increased neuromuscular remodeling with age, as indicated by regionalization of motor nerve terminals (16). In contrast to the EDL muscle in the present study, no increased NCAM immunoreactivity is visible histochemically in 24-month-old mouse soleus muscle, indicating that age-related muscle fiber denervation is most likely specific to individual muscles (16).

Available evidence suggests that muscle fiber denervation and reinnervation is a lifelong, ongoing process that accelerates with aging (16,22). Peripheral axotomy occurs with increased frequency as a result of aging (19). The increasing size of slow motor units and decreasing numbers of fast-fatigable motor units in muscles with mixed fiber types suggests that there may be a loss of fast motor neurons in old animals with subsequent reinnervation of denervated muscle fibers by means of sprouting from slow motor axons (38,39). Though axonal regeneration and reinnervation are maintained throughout life, they are delayed and less effective with increased age (40–42). In addition, in muscles of old animals, decreases in motor unit expansion and indications of impaired Schwann cell–axon interaction are observed during reinnervation (43,44). With aging, neuromuscular junctions exhibit significant morphological change, with increases in area, length, and branch number (45). Forced expansion of the motor unit by means of partial denervation is slower in old muscle and results in 30% fewer normal junctions with associated myelinated axon (43). Reduced motor endplate potential amplitudes are seen in myoneural junctions of old muscles; interestingly the motor endplate potential amplitudes in the “parent” fiber nondenervated junctions are significantly less in old muscle in a partial denervation model (40). These findings indicate impaired reinnervation of denervated muscle fibers in old animals (40,43,44). After a sciatic nerve crush, NCAM expression level for the EDL muscle transiently rises by day 3 but returns to normal values by 11 days; choline acetyltransferase (ChAT) activity at 11 days is interpreted as showing that the muscle is fully reinnervated (34). However, it is not known whether the reinnervated endplate is normal functionally. We suggest that denervation with impaired reinnervation in the muscles from old animals leads to an increased number of functionally denervated fibers and a number of innervated fibers with myoneural junctions that

function marginally. The observed upregulation of NCAM mRNA expression in muscles from old animals is indirect evidence supporting the functional denervation (17). Muscle fibers with impaired reinnervation might label negatively for NCAM protein but still not contract with normal specific force. However, to present a balanced summary, we mention that others have eliminated myoneural junction deficits as a location for the aging force deficit by directly comparing stimulated muscle forces to forces produced by stimulation through the nerve (9).

Despite the many strengths of this aging model, we acknowledge possible limitations. We found no age effect in our comparisons of body mass, muscle mass,  $L_o$ ,  $L_f$ , and CSA (Table 1). However, the muscle mass/body mass ratio is considerably different, being 0.46 and 0.39 mg/g in the YA and OA groups, respectively. This indicates an age-associated increase in 23-month-old F344 rat body fat averaging 14.02% up from 8.6% in 3 month olds; however, the EDL muscle fails to increase in mass, possibly as a result of the lack of functional demand (46,47). Additionally, the statistical power needed to recognize age differences if they existed was below the generally acceptable value (power = 0.80) for morphology variables: muscle mass,  $L_m$ ,  $L_f$ , EDL CSA, CSA<sub>innervated</sub>, and total fiber count when  $\beta = 0.20$ , a priori. Therefore, as we found no significant age differences, it is possible we committed a type II error in failing to reject the null hypotheses for these variables. And finally, only two age groups were studied; we cannot describe fiber innervation in the time spanning our YA to our OA age group. We studied the denervation effect only in the EDL muscle; whether other muscles exhibit the same trend is unknown.

### Conclusions

Increases in muscle fiber denervation accounted for 11.3% of the  $sF_o$  difference between normal YA and OA skeletal muscle. Aging effected a 4.6% decrease in the CSA of EDL muscle, which was composed of innervated muscle fibers. These data support our hypothesis that muscle fiber denervation accounts for some of the  $sF_o$  deficit that occurs with aging. However, other mechanisms for age-related deficits in muscle strength remain undetermined.

### ACKNOWLEDGMENTS

This work was supported by the National Institute of Neurological Disorders and Stroke Grant NS 34380. Dr. Kalliainen received support from the Plastic Surgery Educational Foundation. This work was presented in preliminary form at the Annual Meeting of the Plastic Surgery Research Council, St. Louis, MO, 1996.

Dr. Kuzon has an appointment as a Staff Surgeon, Surgical Service, Department of Veterans Affairs Medical Center, as an Associate Professor of Surgery at The University of Michigan, Ann Arbor, MI. Dr. Kalliainen's current position is Fellow in Hand Surgery, Sections of Plastic and Orthopedic Surgery, University of Virginia, Charlottesville, VA. Ms. Pickens is currently a medical student at the Mayo Medical School, Rochester, MN.

Address correspondence to Dr. M.G. Urbancsek, Department of Surgery, University of Michigan, 2130 Taubman Health Care Center, 1500 E. Medical Center Drive, Ann Arbor, MI 48109-0340. E-mail: melurban@umich.edu

### REFERENCES

1. Brooks SV, Faulkner JA. Contractile properties of skeletal muscles from young, adult and aged mice. *J Physiol (London)*. 1988;404:71–82.
2. Brooks SV, Faulkner JA. Forces and powers of slow and fast skeletal

- muscles in mice during repeated contractions. *J Physiol (London)*. 1991;436:701–710.
3. Lodder MAN, De Haan A, Lind A, Sargeant AJ. Changes in morphological and functional characteristics of male rat EDL muscle during growth. *J Musc Res Cell Motil*. 1993;14:47–53.
  4. Brooks SV, Faulkner JA. Isometric, shortening, and lengthening contractions of muscle fiber segments from adult and old mice. *Am J Physiol*. 1994;267(*Cell Physiol*. 36):C507–C513.
  5. Bruce SA, Newton D, Woledge RC. Effect of age on voluntary force and cross-sectional area of human adductor pollicis muscle. *Q J Exp Physiol*. 1989;74:359–362.
  6. Degens H, Hoofd L, Binkhorst RA. Specific force of the rat plantaris muscle changes with age, but not with overload. *Mech Ageing Dev*. 1995;78:215–219.
  7. Phillips SK, Bruce SA, Newton D, Woledge RC. The weakness of old age is not due to failure of muscle activation. *J Gerontol Med Sci*. 1992;47:M45–M49.
  8. Phillips SK, Wiseman RW, Woledge RC, Kushmerick MJ. Neither changes in phosphorus metabolite levels nor myosin isoforms can explain the weakness in aged mouse muscle. *J Physiol (London)*. 1993;463:157–167.
  9. Brown M, Hasser EM. Complexity of age-related change in skeletal muscle. *J Gerontol Biol Sci*. 1996;51A:B117–B123.
  10. Jubrias SA, Odderson IR, Esselman PC, Conley KE. Decline in isokinetic force with age: muscle cross-sectional area and specific force. *Pflügers Archiv*. 1997;434:246–253.
  11. Phillips SK, Bruce SA, Woledge RC. In mice, the muscle weakness due to age is absent during stretching. *J Physiol (London)*. 1991;437:63–70.
  12. Larsson L, Salviati G. Effects of age on calcium transport activity of the sarcoplasmic reticulum in fast- and slow-twitch rat muscle fibers. *J Physiol (London)*. 1989;419:253–264.
  13. Delbono O, O'Rourke KS, Ettinger WH. Excitation-calcium release uncoupling in aged single human skeletal muscle fibers. *J Membrane Biol*. 1995;148:211–222.
  14. Vandervoort AA, McComas AJ. Contractile changes in opposing muscle of the human ankle joint with aging. *J Appl Physiol*. 1986;61:361–367.
  15. Larsson L, Ansved T, Edström L, Gorza L, Schiaffino S. Effects of age on physiological, immunohistochemical and biochemical properties of fast-twitch single motor units in the rat. *J Physiol (London)*. 1991;443:257–275.
  16. Kobayashi H, Robbins N, Rutishauser U. Neural cell adhesion molecule in aged mouse muscle. *Neuroscience*. 1992;48:237–248.
  17. Andersson AM, Olsen M, Zhernosekov K, et al. Age-related changes in expression of the neural cell adhesion molecule in skeletal muscle: a comparative study of newborn, adult and aged rats. *Biochem J*. 1993;290:641–647.
  18. Larsson L, Ansved T. Effects of ageing on the motor unit. *Progr Neurobiol*. 1995;45:397–458.
  19. Wineinger MA, Sharman RB, Stevenson TR, Carlsen RC, McDonald RB. Peripheral nerve and muscle function in the aging Fischer 344/Brown-Norway rat. *Growth Dev Aging*. 1995;59:107–119.
  20. Covault J, Sanes JR. Neural cell adhesion molecule (N-CAM) accumulates in denervated and paralyzed skeletal muscles. *Proc Natl Acad Sci USA*. 1985;82:4544–4548.
  21. Olsen M, Zuber C, Roth J, Linnemann D, Bock E. The ability to re-express polysialylated NCAM in soleus muscle after denervation is reduced in aged rats compared to young adult rats. *Int J Devl Neurosci*. 1995;13:97–104.
  22. Covault J, Sanes JR. Distribution of N-CAM in synaptic and extrasynaptic portions of developing and adult skeletal muscle. *J Cell Biol*. 1986;102:716–730.
  23. Mendez J, Keys A. Density and composition of mammalian muscle. *Metabolism*. 1960;9:184–188.
  24. Roy RR, Meadows ID, Baldwin KM, Edgerton VR. Functional significance of compensatory overloaded rat fast muscle. *J Appl Physiol*. 1982;52:473–478.
  25. Cote C, Faulkner JA. Motor unit function in skeletal muscle autografts of rats. *Exp Neurol*. 1984;84:292–305.
  26. Institute of Laboratory Animals Resources. *Guide for the Care and Use of Laboratory Animals*. 7th ed. Washington, DC: National Academy Press; 1996.
  27. Faulkner JA, Niemeyer JH, Maxwell LC, White TP. Contractile properties of transplanted extensor digitorum longus muscles of cats. *Am J Physiol*. 1980;238(*Cell Physiol*. 7):C120–C126.
  28. Close R. Dynamic properties of fast and slow skeletal muscles of the rat during development. *J Physiol (London)*. 1964;173:74–95.
  29. Maxwell LC, Faulkner JA, Hyatt GJ. Estimation of the number of fibers in guinea pig skeletal muscle. *J Appl Physiol*. 1974;37:259–264.
  30. Kalliainen LK, Cederna PS, Kuzon WM Jr. Mechanical function of muscle reinnervated by end-to-side neurotomy. *Plast Reconstr Surg*. 1999;103:1919–1927.
  31. Sanes JR, Hall ZW. Antibodies that bind specifically to synaptic sites on muscle fiber basal lamina. *J Cell Biol*. 1979;83:357–370.
  32. Segal SS, White TP, Faulkner JA. Architecture, composition, and contractile properties of rat soleus muscle grafts. *Am J Physiol*. 1986;250(*Cell Physiol*. 19):C474–C479.
  33. Rovak JM, Cederna PS, Macionis V, Urbanchek MS, Van Der Meulen JH, Kuzon WM Jr. Termino-lateral neurotomy: the functional axonal anatomy. *Microsurgery*. 2000;20:6–14.
  34. Daniloff JK, Levi G, Grumet M, Rieger F, Edelman GM. Altered expression of neuronal cell adhesion molecules induced by nerve injury and repair. *J Cell Biol*. 1986;103:929–945.
  35. Rieger F, Grumet M, Edelman GM. N-CAM at the vertebrate neuromuscular junction. *J Cell Biol*. 1995;101:285–293.
  36. Sanes JR, Apel ED, Burgess RW, et al. Development of the neuromuscular junction: genetic analysis in mice. *J Physiol (Paris)*. 1998;92:167–172.
  37. Schäfer R, Wernig A. Polyclonal antibodies against NCAM reduce paralysis-induced axonal sprouting. *J Neurocytol*. 1998;27:615–624.
  38. Kadhiresan VA, Hassett CA, Faulkner JA. Properties of single motor units in medial gastrocnemius muscles of adult and old rats. *J Physiol (London)*. 1996;493:543–552.
  39. Sullivan VK, Powers SK, Criswell DS, Tumer N, Larochelle JS, Lowenthal D. Myosin heavy chain composition in young and old rat skeletal muscle: effects of endurance exercise. *J Appl Physiol*. 1995;78:2115–2120.
  40. Jacob JM, Robbins N. Differential effects of age on neuromuscular transmission in partially denervated mouse muscle. *J Neurosci*. 1990;10:1522–1529.
  41. Verdú E, Butí M, Navarro X. The effect of aging on efferent nerve fibers regeneration in mice. *Brain Res*. 1995;696:76–82.
  42. Carlson BM, Faulkner JA. Reinnervation of long-term denervated rat muscle freely grafted into an innervated limb. *Exp Neurol*. 1988;102:50–56.
  43. Jacob JM, Robbins N. Age differences in morphology of reinnervation of partially denervated mouse muscle. *J Neurosci*. 1990;10:1530–1540.
  44. Kawabuchi M, Chongjian Z, Islam ATMS, Hirata K, Nada O. The effect of aging on the morphological nerve changes during muscle reinnervation after nerve crush. *Restor Neurol Neurosci*. 1998;13:117–127.
  45. Andonian MH, Fahim MA. Effects of endurance exercise on the morphology of mouse neuromuscular junctions during ageing. *J Neurocytol*. 1987;16:589–599.
  46. Mitchell ML, Byrnes WC, Mazzeo RS. A comparison of skeletal muscle morphology with training between young and old Fischer 344 rats. *Mech Ageing Devel*. 1990;58:21–35.
  47. Schoeffner DJ, Warren DA, Muralidhara S, Bruckner JV. Organ weights and fat volume in rats as a function of strain and age. *J Toxicol Environ Health*. 1999;56(Part A):449–462.

Received July 17, 2000

Accepted November 20, 2000

Decision Editor: Edward J. Masoro, PhD